Scilight

Smart Chemical Engineering

https://www.sciltp.com/journals/sce

Article

Light-Triggered Phase Separation of Pickering Emulsions Co-Emulsified by Amino-Functionalized SiO_2 and Spiropyran-Based Ionic Liquid Surfactants

Pengge Chang, Liufang Zhao, Wenwen Li, Yunlei Shi * and Zhiyong Li *

Henan Key Laboratory of Green Chemistry, Collaborative Innovation Center of Henan Province for Green Manufacturing of Fine Chemicals, Key Laboratory of Green Chemical Media and Reactions, Ministry of Education, School of Chemistry and Chemical Engineering, Henan Normal University, Xinxiang 453007, China

* Correspondence: shiyunlei@htu.edu.cn (Y.S.); yli@htu.edu.cn (Z.L.)

How To Cite: Chang, P.; Zhao, L.; Li, W.; et al. Light-Triggered Phase Separation of Pickering Emulsions Co-Emulsified by Amino-Functionalized SiO_2 and Spiropyran-Based Ionic Liquid Surfactants. *Smart Chemical Engineering* **2026**, *2*(2), 6. https://doi.org/10.53941/sce.2026.100006

Received: 4 May 2026
Revised: 10 June 2026
Accepted: 22 June 2026
Published: 25 June 2026

Abstract: Pickering emulsions have demonstrated remarkable potential as a platform for interfacial catalysis. However, the development of simple and efficient strategies to accomplish the objectives of product separation, catalyst recovery, and emulsifier reuse remains an ongoing challenge. In this work, a class of light-responsive Pickering emulsions comprising a spiropyran-based ionic liquid surfactant (SPIL), amino-functionalized SiO_2 (SM-NH_2), toluene, and water was demonstrated, wherein the transition between emulsification and demulsification is reversibly regulated by visible and UV light. Upon visible light irradiation, the SPIL isomerizes from hydrophilic open-ring (MC) to hydrophobic closed-ring (SP), this kind of property change enhances its adsorption onto SM-NH_2, increases zeta potential of the system, and drives the SPIL toward the toluene phase, ultimately leading to demulsification. Conversely, UV light triggers the reverse isomerization, establishing new electrostatic equilibrium with SM-NH_2 to form stable Pickering emulsions. This feature enables the Pickering emulsion to serve as a light-controlled interfacial catalytic microreactor for the hydrolysis of 4-nitrophenyl palmitate. Compared with an aqueous system, this system achieves a 10-fold increase in ester hydrolyze conversion efficiency. It facilitates product separation and allows for the simple recycling of both the emulsifier and the catalyst.

Keywords: pickering emulsion; light switchable; phase separation; reversible emulsification/demulsification; spiropyran

1. Introduction

Since their recognition over a century ago [1,2], Pickering emulsions, stabilized by colloidal particles with suitable wettability [3,4], have gained significant attention. Owing to their high stability and the provision of a large reaction interface, they have been increasingly employed in interfacial catalysis in recent years [5–7]. However, the very stability that makes Pickering emulsions attractive also poses challenges for post-reaction product separation [8,9]. To address this, the development of a simple and sustainable strategy enabling product separation and catalyst recycling, while preserving the interfacial catalytic function, is highly desirable [10]. Such a goal necessitates emulsifiers capable of modulating emulsion behavior on demand. Consequently, stimuli-responsive Pickering emulsions, that can respond to environmental changes, have emerged as a topic of growing interest [11].

In recent years, significant efforts have been dedicated to the development of stimuli-responsive Pickering emulsions, leading to advancements in pH-[12,13], temperature-[14–16], CO_2-[17–19], redox-[20,21] and light-[22–24]

stimulus to tune and control the microstructure and stability of Pickering emulsions. In generally, stimuli-responsive Pickering emulsions can undergo on-demand demulsification or phase inversion, thereby facilitating efficient catalyst recovery. However, when simultaneous product separation, catalyst recovery, and emulsifier recycling are required, the stimulus response must be reversible to enable seamless switching between demulsification and re-emulsification processes, or between oil-in-water (O/W) and water-in-oil (W/O) emulsion types [23].

Among these triggers, light irradiation has clean and non-invasive characteristics, allowing for remote and precise delivery in both time and space [25–27]. The recent years have witnessed obvious advancements in the research of light-responsive Pickering emulsions. The functionalization of spiropyran nanoparticles was employed to create a light-triggered Pickering emulsion. Reversible phase inversion was achieved under near-infrared and visible light irradiation, enabling the utilization of the system for biphasic enantioselective biocatalysis [22]. Interestingly, the reversible phase inversion of the Pickering emulsion facilitated simultaneous product separation as well as catalyst and emulsifier recycling. Similarly, spiropyran modified hollow mesoporous silica nanosphere could form a light-switchable Pickering emulsion. Under UV light irradiation the stable system was demulsified, and it could be re-emulsified under further visible light irradiation [28]. Light-switchable O/W Pickering emulsions were constructed using a SPIL surfactant and UiO-66-NH_2 [24]. The systems underwent reversible emulsification/demulsification under UV/visible light, enabling interfacial catalysis for Click reactions. This system reduces the activation energy from 33.6 to 8.5 kJ/mol and improves conversion by >50%, attributed to spiropyran isomerization that modulates surfactant adsorption and surface activity. The introduction of azobenzene-modified silica particle enables the formation of a light-responsive Pickering emulsion, wherein the application of either UV or blue light induces a reversible transition between water-in-oil droplets and separate water and oil phases [29]. Co-emulsification of light-switchable ionic liquid surfactants and silica microspheres stabilizes a light-responsive Pickering emulsion. Under alternating UV/visible light irradiation, this system underwent reversible emulsification and demulsification, enabling room-temperature hydrogenation of unsaturated hydrocarbons with simultaneous in situ separation of catalysts and products [23].

Silica (SiO_2) is a cost-effective and readily synthesized material with broad applicability, ranging from catalyst supports and biomedical materials to drug delivery systems, coatings, and cosmetics [30–33]. Compared to other inorganic materials, SiO_2 offers favorable biocompatibility, high mechanical stability, and strong corrosion resistance, making it a widely used emulsifier for Pickering emulsions [34]. Lipases are triacylglycerol acyl-hydrolases characterized by a wide operating temperature range, good pH tolerance, and high substrate specificity [35]. Their applications in pharmaceuticals, food, and chemicals are predominantly conducted in aqueous media, and most established catalytic mechanisms of lipases are based on aqueous-phase reactions [36]. Typically, lipases catalyze the hydrolysis of lipids to produce alcohols or acids [37], however, many lipid substrates are poorly water-soluble, necessitating stirring, surfactants, or cosolvents to enhance solubility. Pickering emulsions overcome this limitation by increasing lipid solubility and providing an oil–water interface, where lipases become activated and their active sites are exposed, thereby significantly improving catalytic efficiency [38].

Leveraging the inherent affinity between the amino groups on functionalized SiO_2 (SM-NH_2) and lipase, which is driven by the structural features of the enzyme, in this work, the photo-responsive SPILs ([C_4SPDMEA]Br, [C_6SPDMEA]Br or [C_8SPDMEA]Br, see the structure in Figure 1a) with SM-NH_2 were co-assembled to form stable Pickering emulsions. The system acts as the microreactor for lipase-catalyzed lipid hydrolysis, and the oil–water interface enhances the catalytic efficiency. Compared with the blank experiment, the conversion efficiency of lipid hydrolysis in the Pickering emulsion system is 10 times higher. The system can be reversibly switched between emulsification and demulsification by alternating visible and UV light irradiation (Figure 1b). Therefore, it enables the separation of products and the recycling of both the emulsifier and the catalyst.

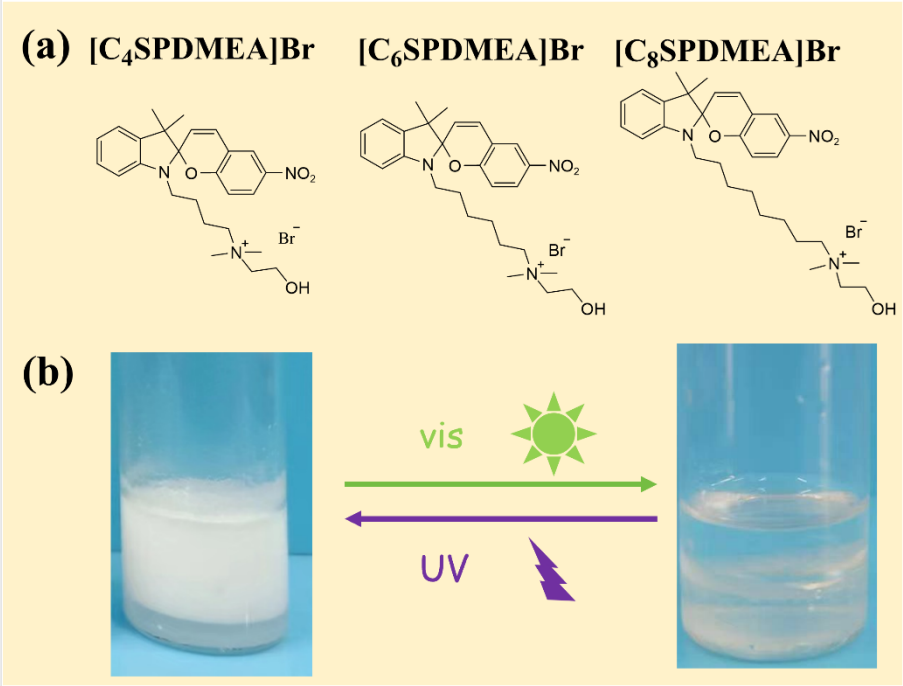

Figure 1. (**a**) Chemical structure of SPILs; (**b**) Photograph depicting the light-induced reversible phase separation of a Pickering emulsion containing SPIL and SM-NH_2.

2. Experimental Section

2.1. Materials

Tetraethyl orthosilicate (TEOS, 98%), 3-(2-aminoethylamino)propyltriethoxysilane (98%), 4-nitrophenyl palmitate (98%), and 4-nitrophenol (99.5%) were purchased from Shanghai Aladdin Scientific Company. Lipase (≥700 U/mg) was purchased from Sigma-Aldrich (St. Louis, MO, USA). The SPILs [C_nSPDMEA]Br (n = 4, 6, 8) were synthesized according to the methodology described in our previous work [24]. All reagents were used directly unless specifically mentioned elsewhere.

2.2. Synthesis of SM-NH_2

SiO_2 microspheres were synthesized following a reported method [39]. Typically, 150 mL of ethanol, 37.5 mL of deionized water, and 8.4 mL of ammonium hydroxide were mixed under stirring at room temperature for 30 min to obtain a homogeneous solution. Subsequently, 6.24 g of TEOS was added to the above solution, and the mixture was stirred continuously for 12 h. The resulting product was collected by centrifugation, washed several times with deionized water, and dried under vacuum at 60 °C for 6 h to yield SiO_2 microspheres (SM).

For the preparation of amino-functionalized silica (SM-NH_2), 0.5 g of the as-prepared SM was dispersed in 5 mL of toluene under a nitrogen atmosphere. Then, 1.55 mmol of 3-(2-aminoethylamino)propyltriethoxysilane was added to the dispersion. The reaction mixture was first stirred at 90 °C for 2 h, followed by further reaction at 110 °C for another 2 h. After the reaction, the solid was collected by centrifugation, washed several times with toluene, and dried in a vacuum oven at 60 °C for 6 h to obtain SM-NH_2. The successful synthesis SM-NH_2 was determined by X-ray photoelectron spectroscopy (XPS), and the results were shown in Figure S1. The binding energy at 399 eV corresponding the introduction of -NH_2 on SiO_2.

2.3. Preparation and Characterization of Pickering Emulsions

For a typical experiment, 1 mL of 1×10^{-4} mol/kg [C_6SPDMEA]Br aqueous solution was placed into a screw-cap vial. Subsequently, 1 mL of 0.5 wt.% SM-NH_2 solution was added to the above system, followed by the addition of 3 mL of toluene. The mixture was homogenized using a homogenizer at 10,000 rpm for 1 min to obtain a Pickering emulsion. The stability of the emulsion was monitored under static conditions. Emulsions that remained stable without phase separation for one week were considered stable Pickering emulsions. The emulsion type was determined by the droplet method, and droplet sizes were observed and recorded using an optical microscope (DYP-990).

2.4. Phase Behavior Reversible Regulation of Pickering Emulsions

The stable Pickering emulsion was irradiated with visible light (20 W, LED) at 25 °C for 10 min under stirring, leading to complete demulsification. Subsequently, the system was irradiated with a cold UV lamp (100 mW/cm^2, 365 nm) for 3 min, followed by re-homogenization. This resulted in re-emulsification and the formation of a stable Pickering emulsion again. The cyclability of the reversible phase behavior of the Pickering emulsion was evaluated by repeating the above procedures.

2.5. Initial Enzymatic Reaction and Conversion Measurement

Typically, 1 mL of enzyme aqueous solution (5 mg/mL), 1 mL of 4-nitrophenyl palmitate in toluene (3 mg/mL), 1 mL of 1 × 10^{-4} mol/kg SPIL aqueous solution, 1 mL of SM-NH_2 (0.5 wt.%), and 3 mL of toluene were added into a screw-cap vial. The mixture was homogenized using a homogenizer at 10,000 rpm for 1 min to obtain a stable Pickering emulsion, which was then placed at 38 °C for 8 h to allow the enzymatic reaction to proceed. After the reaction, the emulsion was completely demulsified by irradiation with visible light under stirring. The oil phase was collected to measure its absorbance, and the conversion of lipid hydrolysis was calculated.

2.6. Recyclability Evaluation of the Pickering Emulsion-Based Catalytic System

The recyclability of the catalytic performance was evaluated using the above system. Under fixed Pickering emulsion composition and enzymatic reaction conditions, after each reaction cycle, the system was irradiated with visible light to achieve complete demulsification. The enzyme catalyst and SM-NH_2 precipitated in the aqueous phase, while the SPIL transferred to the oil phase. However, compared to the concentration of the unreacted lipid, the concentration of the SPIL was too low to affect the absorption peaks in the UV-Vis spectrum of the lipid. The oil phase was collected to measure its absorbance, and the lipid hydrolysis conversion was calculated. The precipitated enzyme catalyst and SM-NH_2 were collected, and a certain amount of SPIL aqueous solution and the lipid solution in toluene were added. The mixture was homogenized again to reform the emulsion for the next enzymatic reaction cycle. The recyclability evaluation was repeated following the same procedures as described above.

3. Results and Discussion

3.1. Evaluation of the Ability to Form Pickering Emulsions

In this work, [C_4SPDMEA]Br, [C_6SPDMEA]Br, and [C_8SPDMEA]Br, were selected together with SM-NH_2 as co-emulsifiers to investigate the feasibility of forming Pickering emulsions in the SPIL/SM-NH_2/toluene/water system. The effects of SPIL structure, SPIL concentration, and SM-NH_2 dosage on the stability of the resulting Pickering emulsions were examined via orthogonal experiments. As shown in Tables S1–S3, SM-NH_2 alone failed to form a stable Pickering emulsion in the absence of SPILs. Upon the addition of SPILs, stable Pickering emulsions were successfully obtained, indicating that the SPILs act as surfactants. For a given SPIL concentration, the stability of the Pickering emulsion increased with increasing mass concentration of SM-NH_2. Similarly, for a fixed SM-NH_2 dosage, stability of the emulsion increased with increasing SPIL concentration. For example, when the SM-NH_2 dosage was fixed at 0.5 wt.%, the SPIL concentration required to obtain a stable Pickering emulsion decreased from 5 × 10^{-4} to 1 × 10^{-5} mol/kg as the alkyl chain length of the SPIL increased, demonstrating that a longer carbon chain reduces the required SPIL concentration. Conversely, when the SPIL concentration was fixed at 5 × 10^{-4} mol/kg, the required SM-NH_2 concentration decreased from 0.4 wt.% to 0.2 wt.% with increasing SPIL alkyl chain length. Under constant concentrations of both SM-NH_2 and SPIL, the minimum SPIL concentration needed to form a stable Pickering emulsion decreased with increasing carbon chain length, following the order: [C_4SPDMEA]Br > [C_6SPDMEA]Br > [C_8SPDMEA]Br. These results indicate that extending the alkyl chain length of the SPIL facilitates the formation of stable Pickering emulsions.

Representative photographs of the formed Pickering emulsions and optical microscopy images of the droplet sizes are shown in Figure 2. As illustrated in Figure 2a, at a fixed [C_6SPDMEA]Br concentration of 1 × 10^{-4} mol/kg, an increase in the mass concentration of SM-NH_2 led to a more compact droplet packing and enhanced stability of the Pickering emulsion. The droplet sizes of the stable emulsions ranged from 10 to 30 μm (Figure 2b). To understand the effect of carbon chain length and the contents of SM-NH_2 on the average droplet diameter of the Pickering emulsions, the optical microscopy photos of the systems were recorded (Figure S2), and the average diameter of the droplets were analyzed. As shown in Figure S3, the average droplet diameter decreases with both longer SPIL alkyl chains and higher SM-NH_2 concentrations. This result is consistent with the law of Pickering emulsion stability obtained above. Based on the above investigations, the type of Pickering emulsion was characterized using the droplet method. The stable emulsion droplets were separately placed in water and toluene. It was observed that the droplets

dispersed and ruptured in water, whereas they remained intact in toluene (Figure S4), indicating that the prepared Pickering emulsion is of the oil-in-water (O/W) type [40,41]. Moreover, to obtain evidence for the adsorption of SM-NH_2 at the oil–water interface, the microstructure of Pickering emulsion droplets after evaporation of water and toluene were examined using optical microscopy and SEM. As shown in Figure S5a, wrinkled structures after removal of both phases were observed. In combination with the SEM image in Figure S5b, these wrinkles can be identified as being composed of SM-NH_2 particles. This observation confirms that SM-NH_2 particles were indeed adsorbed at the toluene–water interface during Pickering emulsion formation [42,43].

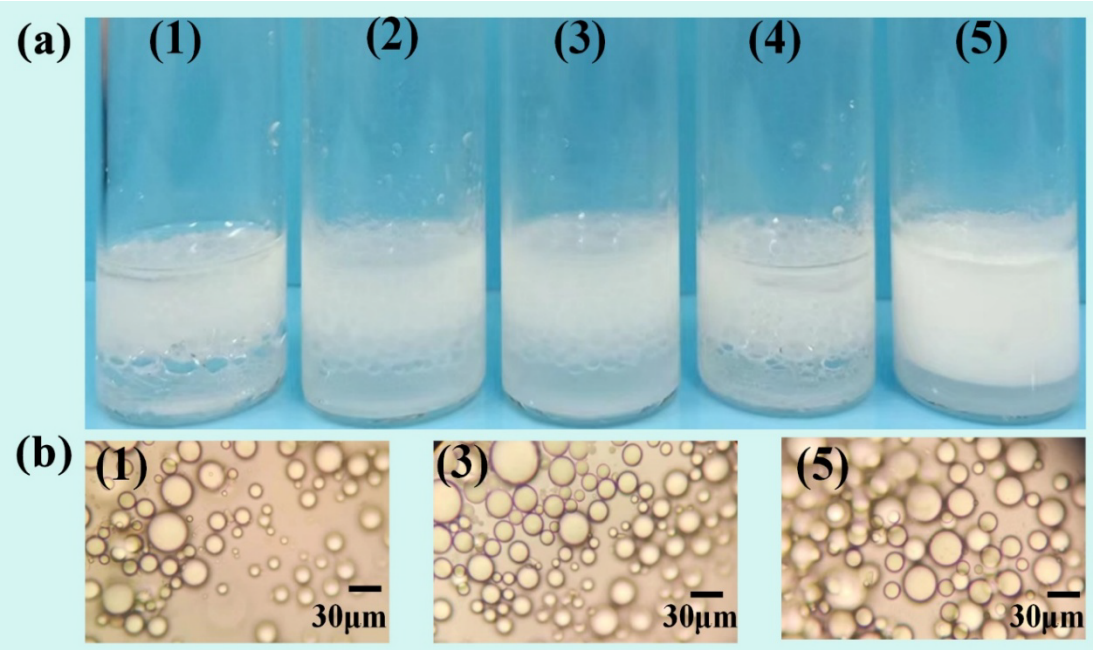

Figure 2. (**a**) Photographs of Pickering emulsions 7 days after preparation containing SM-NH_2, [C_6SPDMEA]Br, toluene and water, the concentration of the SPIL in all samples is 1×10^{-4} mol/kg, from left to right the contents of SM-NH_2, were 0.1%, 0.2%, 0.3%, 0.4%, and 0.5 wt.%, respectively; (**b**) The selected optical micrographs of the [C_6SPDMEA]Br/SM-NH_2/toluene/water with the SPIL concentration of 1×10^{-4} mol/kg for (1), (3) and (5) in (**a**), figures captured after 24 h of standing.

3.2. Light Switchable Phase Behavior of the Pickering Emulsions

The [C_6SPDMEA]Br/SM-NH_2/toluene/water system was selected as a representative example to investigate the emulsification and demulsification behavior under light irradiation. The Pickering emulsion system remained stable without phase separation for more than one week prior to visible light irradiation. Upon irradiation with visible light for 10 min under stirring, phase separation occurred and the emulsion was completely demulsified. Subsequent irradiation with UV light for 3 min led to re-emulsification and the formation of a stable Pickering emulsion, as shown in Figure 1b. Under alternating visible and UV light irradiation, the Pickering emulsion exhibited reversible emulsification and demulsification (Figure 3a). After four cycles, the average droplet diameter was changed from 18.0 μm to 17.6 μm (Figure 3b), this negligible change indicating that the light-responsive Pickering emulsion investigated in this work possesses good reversibility and cyclability. Given that the spiropyran moiety undergoes highly reversible photoisomerization, it is reasonable to expect that the Pickering emulsion can endure more than four cycles.

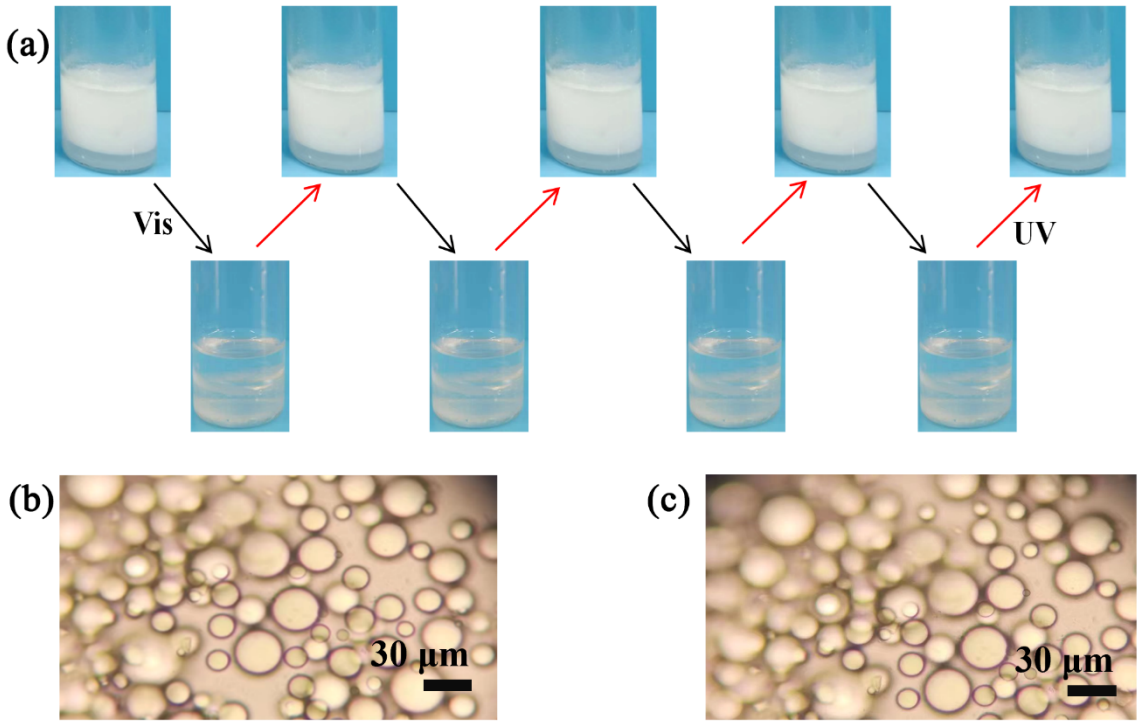

Figure 3. Photographs for fourth cycles of the light-triggered [C_6SPDMEA]Br/SM-NH_2/toluene/water Pickering emulsion reversible emulsification and demulsification (**a**); Optical micrographs of the Pickering emulsion droplets (**b**) before light irradiation and (**c**) after the fourth cycle of visible and UV light irradiation.

3.3. Mechanism of Light Induced Phase Separation of Pickering Emulsions

To investigate the possible mechanism of light induced phase separation of the Pickering emulsion, the Zeta potential and interfacial tension of the [C_6SPDMEA]Br/SM-NH_2/toluene/water system were measured. As shown in Table S4, the Zeta potential of [C_6SPDMEA]Br aqueous solution was 32 mV, while that of the SM-NH_2 (0.5 wt%) aqueous dispersion was 40 mV. Upon the addition of [C_6SPDMEA]Br to the SM-NH_2 dispersion, the Zeta potential decreased to 25 mV. Both the SM-NH_2 and the [C_6SPDMEA]Br system exhibited positive charges, and the electrostatic repulsion between them reached an equilibrium that stabilized the oil–water interface, leading to the formation of a stable Pickering emulsion [4]. Notably, positive zeta potential could be determined for [C_6SPDMEA]Br when the concentration was slightly lower than its CAC [24]. The classic assumption that no aggregates exist below the CAC. In fact, dynamic, positively charged premicellar oligomers are widely present in sub-CAC surfactant systems [44,45]. Such charged species, along with individual surfactant monomers, respond to an applied electric field and produce the detectable zeta potential.

Furthermore, as shown in Table S4, the interfacial tension of the system decreased from 44.13 mN/m to 43.05 mN/m upon the addition of [C_6SPDMEA]Br, indicating that [C_6SPDMEA]Br exhibits a certain degree of surface activity. Together, the SPIL and SM-NH_2 stabilize the immiscible water–toluene two-phase system, resulting in the formation of a Pickering emulsion. Then, the adsorption amount of the SPIL on the SM-NH_2 surface was measured before and after light irradiation. As shown in Figure S6, the adsorption amount increased with increasing [C_6SPDMEA]Br concentration within the investigated concentration range. The adsorption amount after visible light irradiation was higher than that before irradiation. For example, for a [C_6SPDMEA]Br concentration of 1×10^{-4} mol/kg, the adsorption amount increased from 17.91 mmol/g before irradiation to 19.35 mmol/g after irradiation, disrupting the original electrostatic balance at the interface and leading to emulsion demulsification. Moreover, based on our previous work of the partition coefficient of the SPIL in the toluene–water system [24], it is known that under visible light irradiation, the partition coefficient of the SPIL increases, and the SPIL converts from a hydrophilic MC structure to a hydrophobic SP structure. This causes more SPIL to transfer to the toluene phase, resulting in emulsion demulsification.

3.4. Pickering Emulsions for Lipase Catalyzes the Hydrolysis of Lipids

Lipase-catalyzed hydrolysis reactions are common in enzymatic catalysis. However, the catalytic activity of lipases in aqueous systems is generally low due to the inaccessibility of their active sites, resulting in poor hydrolysis conversion efficiency. At an oil–water interface, the α-helix structure covering the active site opens,

exposing the catalytic center and thereby enhancing the hydrolysis conversion [46]. To investigate whether a designed light switchable Pickering emulsion system could improve lipase hydrolysis efficiency, the lipase-catalyzed hydrolysis of 4-nitrophenyl palmitate to 4-nitrophenol was used as a model reaction. The reaction in the aqueous system served as the blank control. In the aqueous system, the hydrolysis conversion efficiency was only 6%, whereas in the Pickering emulsion system, the conversion reached 60%, representing a tenfold increase. These results indicate that in the Pickering emulsion system, the active center of lipase becomes exposed, leading to a significant improvement in the hydrolysis conversion.

The recycling performance of the designed photo-responsive Pickering emulsion was investigated using the lipase-catalyzed hydrolysis of p-nitrophenyl palmitate as a model reaction (see schematic diagram in Figure 4). A stable Pickering emulsion was first formed by homogenizing a toluene-water system containing 4-nitrophenyl palmitate, lipase, SM-NH_2, and [C_6SPDMEA]Br for 1 min. The emulsion was then placed in a water bath at 38 °C and allowed to react for 8 h. After the reaction, the system was exposed to visible light for 20 min to induce complete demulsification under stirring. The product (4-nitrophenol) was partitioned into the aqueous phase, the catalyst precipitated out, and the SPIL transferred to the oil phase. The concentration of SPIL in the upper oil phase (containing unreacted ester) was extremely low and did not interfere with the absorption peak of the ester in the UV-Vis spectrum. The absorbance of the upper oil phase was measured to calculate the ester hydrolysis conversion. The precipitated catalyst was reused in next reaction cycle by adding 3 mL of the ester solution in toluene and 1 mL of the SPIL, followed by homogenization and reaction under the same conditions as before. The recycling results are presented in Figure S7. As the number of cycles increased, the ester hydrolysis conversion gradually decreased, from 60% in the first cycle to about 30% in the third cycle. This decline is likely attributable to significant enzyme loss during the recycling process, leading to poor cycle performance of the system.

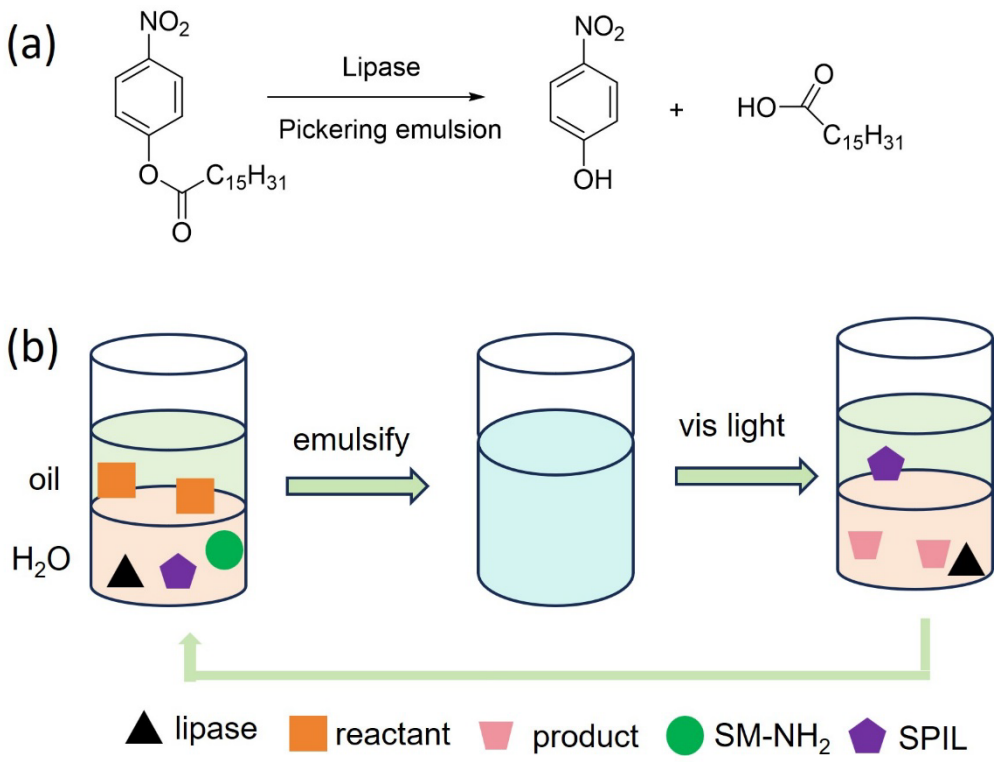

Figure 4. (**a**) Hydrolysis reaction of palmitic acid 4-nitrophenyl ester in Pickering emulsion; (**b**) schematic diagram of the reaction and separation coupling procedures.

4. Conclusions

In summary, we have successfully synthesized functionalized SM-NH_2 and employed them together with SPILs as synergistic emulsifiers to construct a light-responsive Pickering emulsion with water and toluene. Under the irradiation of UV and visible light, emulsification and demulsification of the Pickering emulsion could be reversibly switched. Mechanistic studies reveal that upon UV light irradiation, the SPIL isomerizes from the hydrophobic closed-loop SP form to the hydrophilic open-loop MC form, establishing electrostatic equilibrium with SM-NH_2 and thereby forming a stable Pickering emulsion. In contrast, the open-loop MC structure reverts to the closed-loop SP structure, rendering the SPIL hydrophobic again upon visible light irradiation. This structural

change leads to increased adsorption of the SPIL onto SM-NH_2, an increase in the zeta potential of the system, and enhanced transfer of the SPIL into the toluene phase, ultimately resulting in demulsification of the emulsion. Leveraging the non-invasive, environmentally friendly, and remotely controllable nature of light, these light-responsive Pickering emulsions served as efficient and easily manipulable micro-reactors for chemical reactions. As a demonstration, the system was applied to catalyze the hydrolysis of 4-nitrophenyl palmitate. Compared to a pure aqueous system, the ester conversion in this Pickering emulsion was increased by a factor of 10. This remarkable enhancement is attributed to the large oil–water interface provided by the Pickering emulsion, which exposes the catalytic center of the lipase and significantly improves the conversion efficiency. This innovative strategy effectively integrates emulsion formation, reaction, product separation, and recyclability of both emulsifiers and catalysts in a simple manner, paving the way for the development of sustainable chemical processes.

Supplementary Materials

The additional data and information can be downloaded at: https://media.sciltp.com/articles/others/26062508 52491976/SCE-26050022-SI.pdf. Figure S1: The XPS profiles of SiO_2 and SM-NH_2. Figure S2: The optical microscopy photos of the Pickering emulsions: the concentration of the SPIL is 5×10^{-4} mol/kg, figures captured after fresh preparation. Figure S3: The average droplet diameter by optical microscopy for systems with 5×10^{-4} mol/kg SPIL and varying SM-NH_2 loadings. Figure S4: Photos [C_6SPDMEA]Br/SM-NH_2/toluene/water Pickering emulsion in water (**a**) and toluene (**b**). Figure S5: (**a**) Optical microscopy image of Pickering emulsion droplets after evaporation of water and toluene; (**b**) SEM image of the wrinkled structures from Figure S2a. Figure S6: Adsorption capacity of [C_6SPDMEA]Br on the surface of SM-NH_2 (0.5 wt%) before and after illumination at 25 °C: initial concentration of [C_6SPDMEA]Br, 1×10^{-4} mol/kg; content of SM-NH_2, 0.5 wt%. Figure S7: Conversion efficiency at different cycle numbers. Table S1: Influence of the concentration of [C_4SPDMEA]Br and SM-NH_2 particles in water on the stability of Pickering emulsions formed by [C_4SPDMEA]Br, SM-NH_2, toluene and water. Table S2: Influence of the concentration of [C_6SPDMEA]Br and SM-NH_2 particles in water on the stability of Pickering emulsions formed by [C_6SPDMEA]Br, SM-NH_2, toluene and water. Table S3: Influence of the concentration of [C_8SPDMEA]Br and SM-NH_2 particles in water on the stability of Pickering emulsions formed by [C_8SPDMEA]Br, SM-NH_2, toluene and water. Table S4: The Zeta potential and interfacial tension of [C_6SPDMEA]Br (1×10^{-4} mol/kg) and SM-NH_2 (0.5 wt%) at 25 °C.

Author Contributions

P.C.: investigation, methodology; L.Z.: conceptualization, methodology, data curation; W.L.: investigation, validation; Y.S.: writing—reviewing and editing; Z.L.: supervision, funding acquisition, writing—reviewing and editing. All authors have read and agreed to the published version of the manuscript.

Funding

The authors gratefully acknowledge the financial support from the National Natural Science Foundation of China (No. 22273016), the Natural Science Foundation of Henan Province (No. 252300421043), Plan for Henan Province University Science and Technology Innovation Team (No. 25IRTSTHN002), Young Backbone Teacher Training Program of Henan Province (2023GGJS036), and the 111 project (D17007).

Institutional Review Board Statement

Not applicable.

Informed Consent Statement

Not applicable.

Data Availability Statement

Data is available when requested.

Conflicts of Interest

The authors declare no conflict of interest.

Use of AI and AI-Assisted Technologies

No AI tools were utilized for this paper.

References

1. Ramsden, W.; Gotch, F. Separation of solids in the surface-layers of solutions and 'suspensions' (observations on surface-membranes, bubbles, emulsions, and mechanical coagulation)—Preliminary account. *Proc. R. Soc. Lond.* **1904**, *72*, 156–164. https://doi.org/10.1098/rspl.1903.0034.
2. Pickering, S.U. CXCVI—Emulsions. *J. Chem. Soc. Trans.* **1907**, *91*, 2001–2021. https://doi.org/10.1039/CT9079102001.
3. Yang, H.; Fu, L.; Wei, L.; et al. Compartmentalization of Incompatible Reagents within Pickering Emulsion Droplets for One-Pot Cascade Reactions. *J. Am. Chem. Soc.* **2015**, *137*, 1362–1371. https://doi.org/10.1021/ja512337z.
4. Xu, M.; Jiang, J.; Pei, X.; et al. Novel Oil-in-Water Emulsions Stabilised by Ionic Surfactant and Similarly Charged Nanoparticles at Very Low Concentrations. *Angew. Chem. Int. Ed.* **2018**, *57*, 7738–7742. https://doi.org/10.1002/anie.201802266.
5. Jiang, W.J.; Jiang, H.; Liu, W.; et al. Pickering Emulsion Templated Proteinaceous Microsphere with Bio-Stimuli Responsiveness. *Acta Phys. Chim. Sin.* **2023**, *39*, 2301041. https://doi.org/10.3866/pku.whxb202301041.
6. Ni, L.; Yu, C.; Wei, Q.; et al. Pickering Emulsion Catalysis: Interfacial Chemistry, Catalyst Design, Challenges, and Perspectives. *Angew. Chem. Int. Ed.* **2022**, *61*, e202115885. https://doi.org/10.1002/anie.202115885.
7. Abbas, A.; Hussain, S.; Asad, M.; et al. Pickering emulsion-derived nano/microreactors for unconventional interfacial catalysis: State-of-the-art advances and perspectives in green reactions. *Green Chem.* **2024**, *26*, 3039–3057. https://doi.org/10.1039/d3gc02512h.
8. Pera-Titus, M.; Leclercq, L.; Clacens, J.-M.; et al. Pickering Interfacial Catalysis for Biphasic Systems: From Emulsion Design to Green Reactions. *Angew. Chem. Int. Ed.* **2015**, *54*, 2006–2021. https://doi.org/10.1002/anie.201402069.
9. Jiang, J.; Zhu, Y.; Cui, Z.; et al. Switchable Pickering Emulsions Stabilized by Silica Nanoparticles Hydrophobized In Situ with a Switchable Surfactant. *Angew. Chem. Int. Ed.* **2013**, *52*, 12373–12376. https://doi.org/10.1002/anie.201305947.
10. Schrade, A.; Landfester, K.; Ziener, U. Pickering-type stabilized nanoparticles by heterophase polymerization. *Chem. Soc. Rev.* **2013**, *42*, 6823–6839. https://doi.org/10.1039/c3cs60100e.
11. Tang, J.; Quinlan, P.J.; Tam, K.C. Stimuli-responsive Pickering emulsions: Recent advances and potential applications. *Soft Matter* **2015**, *11*, 3512–3529. https://doi.org/10.1039/C5SM00247H.
12. Yang, H.; Zhou, T.; Zhang, W. A Strategy for Separating and Recycling Solid Catalysts Based on the pH-Triggered Pickering-Emulsion Inversion. *Angew. Chem. Int. Ed.* **2013**, *52*, 7455–7459. https://doi.org/10.1002/anie.201300534.
13. Pei, X.; Zhang, S.; Zhang, W.; et al. Behavior of Smart Surfactants in Stabilizing pH-Responsive Emulsions. *Angew. Chem. Int. Ed.* **2021**, *60*, 5235–5239. https://doi.org/10.1002/anie.202013443.
14. Hwang, Y.-H.; Jeon, K.; Ryu, S.A.; et al. Temperature-Responsive Janus Particles as Microsurfactants for On-Demand Coalescence of Emulsions. *Small* **2020**, *16*, 2005159. https://doi.org/10.1002/smll.202005159.
15. Thompson, K.L.; Fielding, L.A.; Mykhaylyk, O.O.; et al. Vermicious thermo-responsive Pickering emulsifiers. *Chem. Sci.* **2015**, *6*, 4207–4214. https://doi.org/10.1039/c5sc00598a.
16. Li, C.P.; Hu, J.T.; Tang, C.; et al. Thermo-Switchable Pickering Emulsion Stabilized by Smart Janus Nanosheets for Controllable Interfacial Catalysis. *ACS Sustainable Chem. Eng.* **2023**, *11*, 14144–14157. https://doi.org/10.1021/acssuschemeng.3c03703.
17. Pei, X.; Song, W.; Shi, Y.; et al. CO_2-Switchable Emulsification and Demulsification of Pickering Emulsion Stabilized by Zirconium-Based Metal-Organic Frameworks. *ACS Sustainable Chem. Eng.* **2023**, *11*, 796-803. https://doi.org/10.1021/acssuschemeng.2c06446.
18. Li, Z.X.; Shi, Y.L.; Ding, Y.M.; et al. Zr-Based MOF-Stabilized CO_2-Responsive Pickering Emulsions for Efficient Reduction of Nitroarenes. *Langmuir* **2024**, *40*, 3133–3141. https://doi.org/10.1021/acs.langmuir.3c03564.
19. Xi, Y.K.; Liu, B.; Wang, S.X.; et al. CO_2-responsive Pickering emulsions stabilized by soft protein particles for interfacial biocatalysis. *Chem. Sci.* **2022**, *13*, 2884–2890. https://doi.org/10.1039/d1sc06146a.
20. Yang, Y.; Sun, H.; Wang, M.; et al. pH- and Redox-Responsive Pickering Emulsions Based on Cellulose Nanocrystal Surfactants. *Angew. Chem. Int. Ed.* **2023**, *62*, e202218440. https://doi.org/10.1002/anie.202218440.
21. Lu, W.; Dong, J.; Zhang, D.; et al. Redox-switchable Pickering emulsion stabilized by hexaniobate-based ionic liquid for oxidation catalysis. *Dalton Trans.* **2023**, *52*, 6677–6684. https://doi.org/10.1039/d3dt00973d.
22. Chen, Z.; Zhou, L.; Bing, W.; et al. Light Controlled Reversible Inversion of Nanophosphor-Stabilized Pickering Emulsions for Biphasic Enantioselective Biocatalysis. *J. Am. Chem. Soc.* **2014**, *136*, 7498–7504. https://doi.org/10.1021/ja503123m.

23. Li, Z.; Shi, Y.; Zhu, A.; et al. Light-Responsive, Reversible Emulsification and Demulsification of Oil-in-Water Pickering Emulsions for Catalysis. *Angew. Chem. Int. Ed.* **2021**, *60*, 3928–3933. https://doi.org/10.1002/anie.202010750.
24. Li, Z.; Niu, L.; Zhao, L.; et al. Light-Switchable Pickering Emulsions Emulsified by Spiropyran-Based Ionic Liquid Surfactants and UiO-66-NH_2. *ChemSusChem* **2025**, *18*, e202501618. https://doi.org/10.1002/cssc.202501618.
25. Li, Z.; Feng, Y.; Liu, X.; et al. Light triggered switchable ionic liquid aqueous two-phase systems. *ACS Sustainable Chem. Eng.* **2020**, *8*, 15327–15335. https://doi.org/10.1021/acssuschemeng.0c05703.
26. Zhao, L.; Yuan, X.; Wang, H.; et al. Light-switchable emulsions: From reversible emulsification-demulsification to controllable microreactors. *J. Mol. Liq.* **2023**, *372*, 121166. https://doi.org/10.1016/j.molliq.2022.121166.
27. Glikman, D.; Wyszynski, L.; Lindfeld, V.; et al. Charge Regulation at the Nanoscale as Evidenced from Light-Responsive Nanoemulsions. *J. Am. Chem. Soc.* **2024**, *146*, 8362–8371. https://doi.org/10.1021/jacs.3c14112.
28. Zhong, H.Y.; Zhang, Y.; Gong, Y.M.; et al. Ultraviolet/Visible Light-Responsive Pickering Interfacial Biocatalysis: Efficient and Robust Platform for Bioconversions. *ACS Sustainable Chem. Eng.* **2023**, *12*, 1857–1867. https://doi.org/10.1021/acssuschemeng.3c05438.
29. Richards, K.D.; Evans, R.C. Light-responsive Pickering emulsions based on azobenzene-modified particles. *Soft Matter* **2022**, *18*, 5770–5781. https://doi.org/10.1039/d2sm00697a.
30. Knopp, D.; Tang, D.; Niessner, R. Review: Bioanalytical applications of biomolecule-functionalized nanometer-sized doped silica particles. *Anal. Chim. Acta* **2009**, *647*, 14–30. https://doi.org/10.1016/j.aca.2009.05.037.
31. Ki, M.-R.; Kim, J.K.; Kim, S.H.; et al. Compartment-restricted and rate-controlled dual drug delivery system using a biosilica-enveloped ferritin cage. *J. Ind. Eng. Chem.* **2020**, *81*, 367–374. https://doi.org/10.1016/j.jiec.2019.09.027.
32. Bell, N.C.; Minelli, C.; Tompkins, J.; et al. Emerging Techniques for Submicrometer Particle Sizing Applied to Stöber Silica. *Langmuir* **2012**, *28*, 10860–10872. https://doi.org/10.1021/la301351k.
33. Park, K.M.; Kim, S.E.; Lee, B.I.; et al. Top 100 cited articles on epilepsy and status epilepticus: A bibliometric analysis. *J. Clin. Neurosci.* **2017**, *42*, 12–18. https://doi.org/10.1016/j.jocn.2017.02.065.
34. Ki, M.-R.; Yeo, K.B.; Pack, S.P. Surface immobilization of protein via biosilification catalyzed by silicatein fused to glutathione S-transferase (GST). *Bioprocess Biosyst. Eng.* **2013**, *36*, 643–648. https://doi.org/10.1007/s00449-012-0818-x.
35. Dheeman, D.S.; Frias, J.M.; Henehan, G.T.M. Influence of cultivation conditions on the production of a thermostable extracellular lipase from amycolatopsis mediterranei DSM 43304. *J. Ind. Microbiol. Biotechnol.* **2010**, *37*, 1. https://doi.org/10.1007/s10295-009-0643-7.
36. Gandhi, N.N. Applications of lipase. *J. Am. Oil Chem. Soc.* **1997**, *74*, 621–634. https://doi.org/10.1007/s11746-997-0194-x.
37. Brady, L.; Brzozowski, A.M.; Derewenda, Z.S.; et al. A serine protease triad forms the catalytic centre of a triacylglycerol lipase. *Nature* **1990**, *343*, 767–770. https://doi.org/10.1038/343767a0.
38. Gautam, K.K.; Tyagi, V.K. Microbial surfactants: A review. *J. Oleo Sci.* **2006**, *55*, 155–166. https://doi.org/10.5650/jos.55.155.
39. Stöber, W.; Fink, A.; Bohn, E. Controlled growth of monodisperse silica spheres in the micron size range. *J. Colloid Interface Sci.* **1968**, *26*, 62–69. https://doi.org/10.1016/0021-9797(68)90272-5.
40. Ghosh, S.; Rahaman, S.M.; Ghosh, N.G.; et al. Design and formulation of saponin-based, mustard oil-derived, extra stable oil-in-water emulsion: Exploration of its antimicrobial activity. *New J. Chem.* **2026**, *50*, 3607–3614. https://doi.org/10.1039/D5NJ04411A.
41. Rahaman, S.M.; Joshi, D.; Patra, A.; et al. A pH switchable Pickering emulsion stabilised by controlled non-conventional lanthanum sulfide nanoparticles, in situ hydrophobized with a cationic surfactant. *New J. Chem.* **2024**, *48*, 4063–4076. https://doi.org/10.1039/D3NJ04477G.
42. Shi, Y.L.; Xiong, D.Z.; Li, Z.Y.; et al. Ambient CO_2 Switchable Pickering Emulsion Emulsified by TETA-Functionalized Metal-Organic Frameworks. *ACS Appl. Mater. Interfaces* **2020**, *12*, 53385–53393. https://doi.org/10.1021/acsami.0c13157.
43. Zou, H.; Li, Q.; Zhang, R.; et al. Amphiphilic Covalent Organic Framework Nanoparticles for Pickering Emulsion Catalysis with Size Selectivity. *Angew. Chem. Int. Ed.* **2024**, *63*, e202314650. https://doi.org/10.1002/anie.202314650.
44. Cui, X.; Mao, S.; Liu, M.; et al. Mechanism of Surfactant Micelle Formation. *Langmuir* **2008**, *24*, 10771–10775. https://doi.org/10.1021/la801705y.
45. Shimizu, S.; Matubayasi, N. Surface Tension Isotherms: Reconceptualizing Adsorption, Self-Assembly, and Micelle Formation via the Fluctuation Theory. *Langmuir* **2026**, *42*, 5416–5430. https://doi.org/10.1021/acs.langmuir.5c05155.
46. Straathof, A.J.J.; Jongejan, J.A. The enantiomeric ratio: Origin, determination and prediction. *Enzyme Microb. Technol.* **1997**, *21*, 559–571. https://doi.org/10.1016/S0141-0229(97)00066-5.